Indian Journal of Radio & Space Physics
Vol 45, September 2016, pp 101-114

Changes in foF2 parameter in the ionosphere at mid and low latitude before and after earthquake

Harleen Kaur[a]*, Shivali Verma[a] & Pramod Kumar Purohit[b]

[a]Department of Physics, Barkatullah University, Bhopal 462 026, India

[b]National Institute of Technical Teacher's Training and Research, Bhopal 462 002, India

Received 24 February 2016; revised 20 May 2016; accepted 22 September 2016

This paper investigates the ionospheric variations pre and post to the occurrence of four earthquakes of mid and low latitude during 2011-2014. A running median of the foF2 and associated inter- quartile range (IQR), upper bound (UB) and lower bound (LB) are employed as a reference for identifying abnormal signals during all four earthquakes. Our results revealed anomalous reductions and enhancements in the foF2 within 7 days pre and post the earthquakes. The analysis during very quiet geomagnetic conditions is displayed to be a useful indicator of a forthcoming earthquake. A possible mechanism accountable for ionospheric anomalies associated with these earthquakes is discussed.

Keywords: Ionosphere, Anomalies, foF2, Earthquake, Coupling, Perturbations

1 Introduction

The Earth's ionosphere is closely associated to further geospheres. In this regard, the ionosphere can be considered as a natural indicator of disturbances in near-Earth space. Ionospheric state control and anomaly extraction are significant errands of ionospheric parameter investigation[1,2]. Ionospheric parameters touch many spheres of our being and can have a negative effect on satellite arrangements and radio communication transmission. Natural and anthropogenic disorders may source wave annoyances of ionospheric parameters and change the ionospheric dynamics throughout the world. In this context the natural seismo-ionospheric anomalies have been broadly explored in the last two decades[3,4]. In seismically dynamic regions parameters can also be detected in periods of amplified seismic activity[5,6]. The observational signals from the last twenty years provide a noteworthy pattern of passing anomalies preceding tremors[7-11]. At the early of the 1980s, according to the explanations of the ionosphere by vertical sounding stations in seismo active fragments of Middle Asia, it was recommended that the critical frequency foF2 could be adequately sensitive to earthquake preparation developments[12-15]. Such impression had to be verified and basically applied taking into account a number of uninterruptedly working vertical ionospheric sounding stations confined at different locations on earth, among other in seismo-active areas. Pulinets *et al.*[16] applied a statistical method to get a reliable precursor of the earthquake and reported that the perturbations happen just after the shock and are due to acoustic waves, which are enlarged during the atmosphere because of subsiding atmospheric density by increasing height. A lessening of the critical frequency foF2 before a few earthquakes was established by numerous researchers[17-20]. Pulinets & Boyarchuk[3] remarked an enhancement of foF2 before an enormously strong earthquake. A statistical examination of the fo F2-reduction in the afternoon before Taiwan earthquakes was accomplished by Liu *et al.*[21]. These soundings were supported for earthquakes with altered ranges of magnitudes. He saw 20% diminution of foF2 from 0-5 days before earthquakes. Liu *et al.*[22] examined the ionospheric plasma frequency accepted by a local ionosonde and established that the critical frequency of F_2-peak foF2, considerably decreased few days former to most of M>6.0 earthquakes in Taiwan area. During 2002–2010, 736 earthquakes of M>6 around the globe at different latitude and longitude were statically studied, and the feature of LT variation in ionospheric irregularities was established by Le *et al.*[23]. Following the methodology of interquartile range evoked by Liu *et al.*[8] evinced that the ionospheric growth predominantly seemed before earthquakes. Zelenova and Legenka[24] have performed the spectral analysis of the critical

*Corresponding author (E-mail: harleen74@gmail.com)

frequency deviation (ΔfoF2%) for the period of many days prior the Moneron earthquake. The quantitative estimations of the ionosphere unevenness can be seen in the works by many other researchers[25-27], displaying that day to day changeability of the critical frequency foF2 lies within the range 10–30%. So in this paper we have also used the method described by the Liu *et al.*[8] for analysis of earthquakes.

2 Selection of Geographical Region: Low and Mid Latitude

The distribution and characteristics of ionospheric parameter over low, mid, and high latitudes have been probed by authors[28,29]. This work aims at inspecting the ionospheric perturbations prior and post to the earthquakes with a magnitude M6.9-M8.6 over low and mid latitude during the period from 2011–2014 using ionosonde foF2 measurements surrounding the epicenters. The aim of the present work is the statistical analysis of the foF2 for earthquakes located at the given geographical coordinates. The manifestation time, geographic coordinates, magnitude, distance of data receiver station from epicenter and the radius of the earthquake preparation zone of these mid and low latitude events are précised in Table 1. The radius of the earthquake preparation zone for each earthquake is calculated by using the Dobrovolsky formula as $R = 10^{0.43M}$, where R is the radius of the tremor preparation zone in km and M is the earthquake magnitude on the Richter scale[30]. Figure 1 presents the locations of the earthquake epicenters (star) and foF2 data receiver stations (triangle), in geographic coordinates.

3 Data Processing and Measurement Techniques

Ionosonde foF2 data was studied 7 days prior and later to the earthquake and was retrieved from Spidr NOAA. It is found that the ionosphere has strong seasonal, annual, and solar cycle fluctuations; so using a long-term data set to find out the median is not judicious (Xu *et al.*[31]). Hence the running median was calculated over 15 days of data. Under the supposition of normal distribution, the projected value of IQR was 1.34 σ. To detach abnormal signals, we compute running median $\overline{X}$ of foF2 for each hour and the allied Inter Quartile Range (IQR) to construct the upper bound ($\overline{X}$+IQR) and lower bound ($\overline{X}$+IQR). These bounds are intended during the shock periods to better isolate seismic anomalies from natural and seasonal variations by Liu *et al.*[8]. Under the assumption of a normal distribution with median $\overline{X}$ and standard deviation σ for the foF2, the expected

Table 1 – The magnitude, geographic coordinates, distance between data receiver station and the epicenter along with the earthquake preparation zone of the earthquakes (http://earthquake.usgs.gov)

Magnitude (Richter scale)	Date of happening	Geographical coordinates of the epicenter		Geographical coordinates of Data collector station		Dobrovolsky range	Distance between receiver & epicenter
		Lat (°)	Long(°)	Lat (°)	Long(°)		
8.6	April 11, 2012	2.31°N	93.06°E	12.18°S	96.98°E	4989 km	1665 km
8.2	April 1, 2014	19.61°S	70.76°W	12.1°S	77°W	3357 km	1068 km
7.2	June 24, 2011	52.00°N	171.85°W	58.4°N	156.4°W	1250 km	1207 km
6.9	May 24, 2014	40.28°N	25.38°E	38.0°N	23.5°E	927 km	301 km

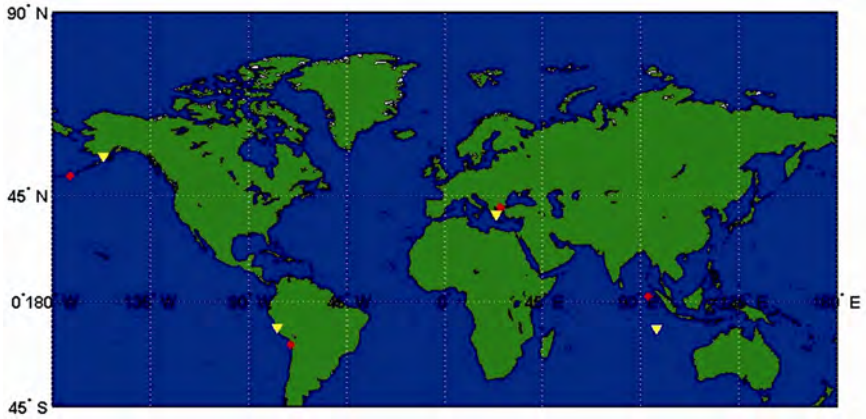

Fig. 1 – Geographic sites of the four earthquake epicenters (red star) and their respective Ionosonde receiver stations (yellow triangle)

value of IQR is 1.34 σ. To yield a stringent criterion, the upper and lower bounds of IQR are estimated using the following formulas:

IQR Upper bound (UB) = $\overline{X}$+1.34 σ ... (1)

IQR Lower bound (LB) = $\overline{X}$-1.34 σ ... (2)

If the foF2 value at this time point was greater than the UB or lesser than LB, it was well-defined as an abnormal point. To quantify the ionospheric disturbances, the percentage of foF2 deviation (ΔfoF2 %) has been studied from, both the upper bound and lower bound. This index offers facts about the negative and positive phases that occur during the earthquake period and can be obtained by means of Eqs (1) and (2) formulated byDabas *et al.*[32] which is called as %deviation positive and %deviation negative:

$$\Delta foF2\% \text{ (positive)} = \frac{foF2_{EQ} - IQR_{UB}}{IQR_{UB}} \times 100$$

If $foF2_{EQ} \leq IQR_{UB}$ then ΔfoF2% (positive) = 0

$$\Delta foF2\% \text{ (negative)} = \frac{foF2_{EQ} - IQR_{LB}}{IQR_{LB}} \times 100$$

If $foF2_{EQ} \geq IQR_{LB}$ then ΔfoF2% (negative) = 0

where $foF2_{EQ}$ is the value of foF2 during earthquake period.

We have observed inconsistent variations of ionospheric foF2 which seems to be associated with earthquake by analyzing foF2 data. Anomalous variation of foF2 is taken be different from hour to hour and day to day variability**.**Ionospheric modification caused by geomagnetic storm activity can support amplification, or weakening, of the manifestation of seismo-ionospheric effects[33]. So it must to analyze Kp, Dst, ap and AE. The ionospheric effect of a geomagnetic storm has a global influence which is observable all over the sphere, while the seismogenic effect is witnessed only by stations with a distance of not more than 2000 km from the epicenter[3,16]. Gonzalez *et al.*[34]agreed that the magnetic storm can develop when the Dst index exceeds the threshold and stay over this onset for at least 2 h. According to Osella*et al.*[35]for the geomagnetic storm to commence the value of Dst Peaks<-30 nT ,ap>30 and AE>1000 nT. To rule-out the possibility of anomaly finding during high and moderate geomagnetic activity, the ΔfoF2% values with |Dst|>15 nT,ap>16 and -3<Kp<3 are filtered out in our analysis. Hence we get quiet period for foF2 analysis. If the appeared anomalies are less than 1%, then such anomalies are neglected in the calculations. The hourly geophysical activities are obtained from World Data Centre Kyoto, seven days pre and post the tremors.

3.1 Analysis of the ionospheric variations of April 11, 2012, Sumatra earthquake

April 11, 2012, M8.6 earthquake at 08:38 universal time UT (/) having depth 22.9 km occurred at the off west coast of Northern Sumatra (2.311°N, 93.063°E), as result of strike-slip faulting within the oceanic lithosphere of the Indo-Australia plate. The quake was positioned 200 km of the southwest of the major subduction zone that expresses the plate boundary between the India/Australia and Sunda plate's offshore Sumatra. Here, the India/Australia plates move north-northeast regarding the Sunda plate at a velocity of approximately 52 mm/y. The data receiver is positioned at CocosIsland (12.18°S, 96.98°E) which is 1665.2 km from the epicenter lies in Dobrovolsky zone, as depicted in Table 1. Figure 2 presents the geomagnetic indices Dst, AE,Kp, ap, and the foF2 variations with the related UB and LB for the examination period between 3 April to 18 April 2012, at data receiver station. The vertical arrow in Fig. 2(c) marks the earthquake time. The horizontal black lines in Fig. 2(a, b) confirms the threshold values of the Dst and ap indices, which are -15 nT and 16, respectively. In Fig. 2(c), foF2 signals derived from ionosonde with the UB and LB are plotted using the method discussed in Section 3. The foF2 signal was successful to surpass the UB and LBs in Fig. 2(c). The detections were seen between the period of 7 days pre and post shock activity at the vicinity of the epicenter. However, as identified by the Dst, AE, Kp and ap indices in Fig. 2(a, b), the geomagnetic conditions during the days of 6 April and 12 April were disturbed, while the geomagnetic levels on 5 April and 15 to 18 April were characterized as quiet. Therefore, only foF2 anomalies observed for this quiet days are reflected as possible pre-earthquake ionospheric anomalies, hence they are highlighted by the *P* character and the ones seen on disturbed days are highlighted by the *D* character as depicted in Fig. 2(c). Figure 3 shows the percentage of foF2 deviation (ΔfoF2%) for the same surveillance period presented in Fig. 2. In this figure, the positive and negative values of the filtered ΔfoF2% validate the variation as compare to the UB and LB, respectively. As exposed in Fig. 3(b), significant increases in ΔfoF2% of about 1–34% were observed on considered quiet days of

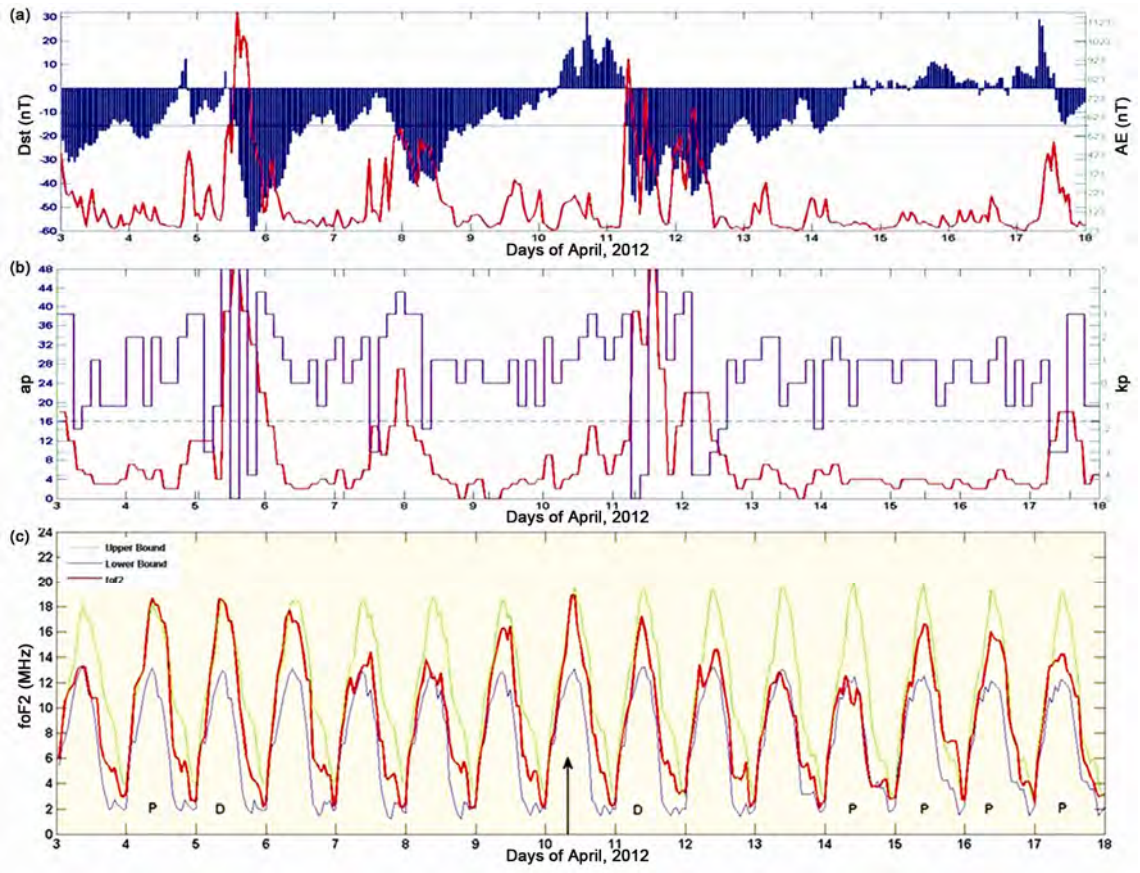

Fig. 2 – The geomagnetic indices (a) Dst and AE (b) ap and Kp, and the (c) foF2 variations and the associated UB and LB between 3 April to 18 April 2012, at the epicenter (2.311°N, 93.063°E), obtained by ionosonde

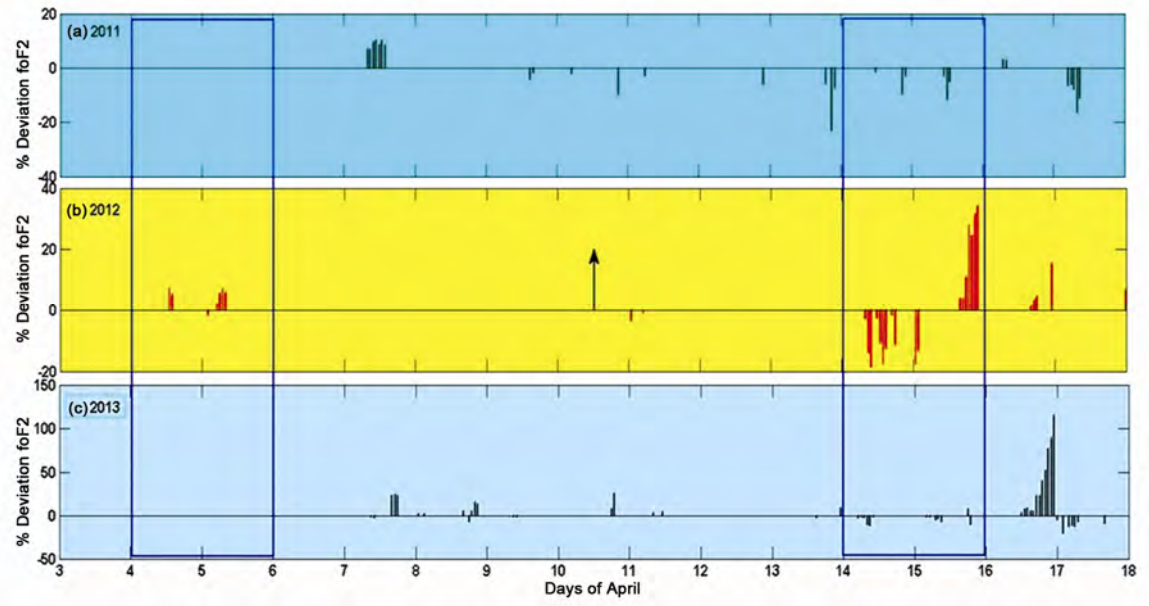

Fig. 3 – Between 3 April to 18 April, 2012 the positive and negative values verify the filtered ΔfoF2% variations with respect to their UB and LB, derived from ionosonde (a) at the (2.311°N, 93.063°E) in 2011; (b) at the epicenter (2.311°N, 93.063°E) in 2012; (c) at the (2.311°N, 93.063°E) in 2013

April with respect to Fig. 2(c). Extreme crest amplification (34%) appears on 16 April, 2012 post to the 5th day of the earthquake occurrence day.

To validate whether these anomalies appeared due to earthquake, we have processed foF2 data pre and post shock years in the same span of observation. Percentage deviation for years 2011 and 2013 are calculated at (2.311°N, 93.063°E) by the same methodology as described in Section 3, which is plotted in Fig. 3(a) and Fig. 3(c), respectively. From Fig. 3(b) it is obvious that anomalies appeared on pre earthquake days which fall on 5-6 April whereas no inconsistencies are visible in Fig. 3(a) and Fig. 3(c). Again after shock day in 2012, extreme negative and extreme positive perturbations appeared on 15 and 16 April, respectively, while very small percentage deviation is witnessed in years 2011 and 2013. Blue block in Fig. 3 marks the noteworthy days. Therefore to find out the local disparity for the extreme crest amplification day we have calculated the variation of foF2 with the UB and LB which is plotted in Fig. 4. It reveals that this variant is corresponding to the anomaly which occurs at 1LT (Local time) to the 5LT (LT=UT+7hr) on 16 April, 2012.

3.2 Analysis of the ionospheric variations of April 1, 2014, IquiqueChile earthquake

April 1, 2014 M8.2 tremor in Northern Chile occurred at of as the result of thrust faulting at low depth near the Chilean coast (19.61°S, 70.76°W) at 23:46 UT (Universal time) having depth 25km. At the latitude of this earthquake, the Nazca plate subducts eastward underneath the South America plate at a rate of 65 mm/y. Subduction alongside the Peru-Chile Trench to the west of Chile has led to elevate the Andes highland range and has produced some of the largest earthquakes like the 2010, M 8.8 Maule earthquake in central Chile and 1960, M9.5 earthquake in Southern Chile. This earthquake happened in a region of historic seismic quiescence, as historic records specify an M8.8 earthquake occurred within the Iquique gap in 1877. The data receiver is located at Jicamarca (12.1°S, 77°W) which is 1068 km from the epicenter and lies in Dobrovolsky zone, as depicted in Table 1. Figure 5 depicts the geomagnetic indices Dst, AE, Kp, ap and the foF2 discrepancies with the linked UB and LB for the observation period between 24 March to 8 April 2014, at data receiver station. The vertical arrow in the figure marks the time of the shock. The horizontal black lines in Fig. 5(a,b) demonstrates the threshold values of the Dst and ap indices, which are -15 nT and 16, respectively. In Fig. 5(c), foF2 signal derived from ionosonde with the UB and LBs are schemed as described in Section 3. This foF2 signal was prolific to beat the UB and LBs in Fig. 5(c). These findings were witnessed between the period of 7 days pre and post shock activity at the vicinity of the epicenter. Nevertheless, as indicated by the Dst, AE, Kp and ap indices in Fig. 5(a,b), the geomagnetic conditions were not disturbed in our study period for this earthquake. Therefore, only foF2 anomalies observed on 25-29 March, 31 March, 1-6 April and 8 April are considered as possible pre-earthquake ionospheric anomalies, hence they are highlighted by the *P* character as depicted in Fig. 5(c). Figure 6 illustrates, significant rises in ΔfoF2% of about 1–19% were observed on 25-29 March, 31 March, 1-6 April and 8 April with respect to Fig. 5(c). Extreme crest amplification (19%) appears on 28 March, 2014, prior to the three days of the earthquake occurrence.

To find out the cause of extreme crest amplification the LT irregularities in the ionosphere of 28 March, 2014 are plotted in Fig. 7. From the Fig. 7 we reveal that the discrepancy in foF2 from its UB started from

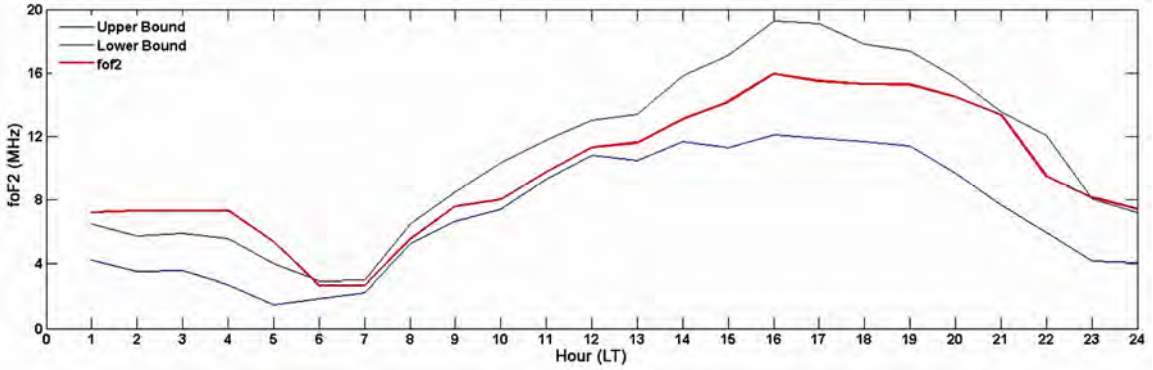

Fig. 4 – LT variations in foF2, UB, LB on 16April, 2012

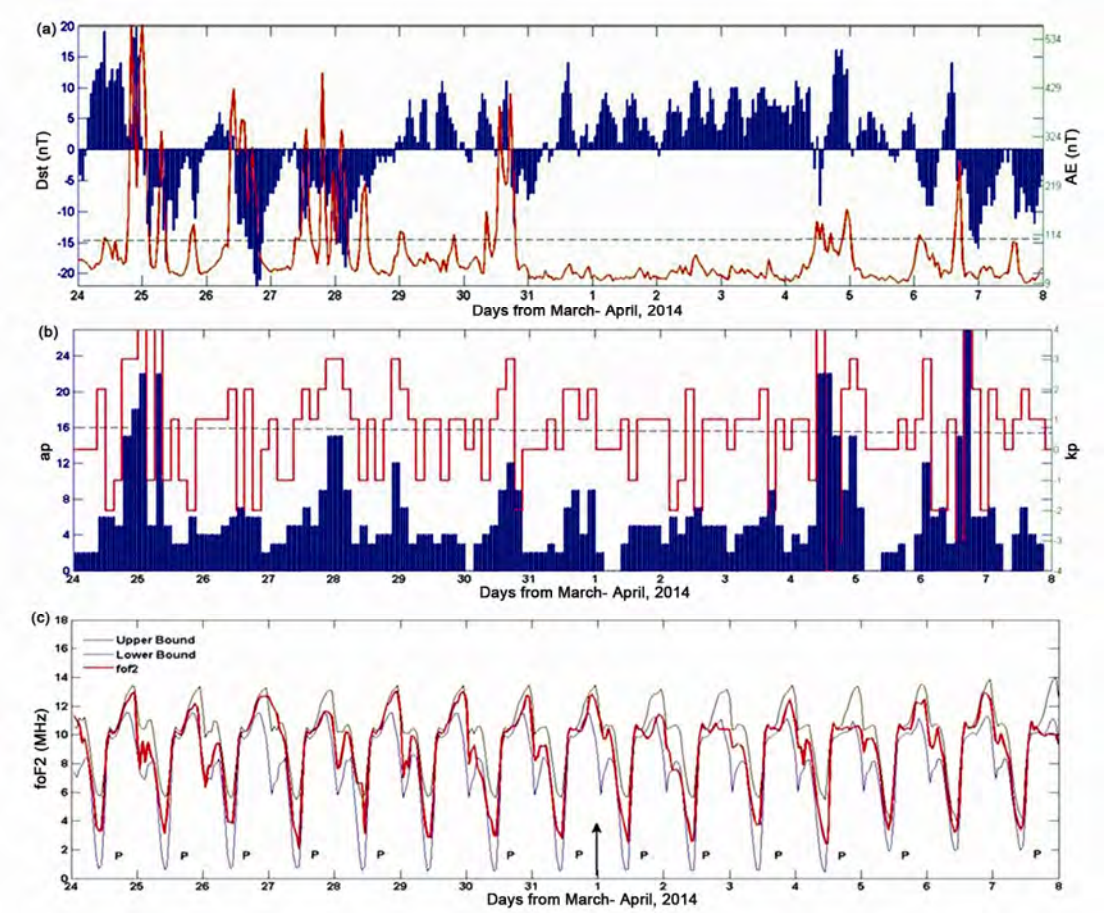

Fig. 5 – The geomagnetic indices (a) Dst and AE, (b) ap and Kp, and the (c) foF2 variations and the linked UB and LB between 24 March to 8 April 2014, at the epicenter (19.61°S, 70.76°W), obtained by ionosonde

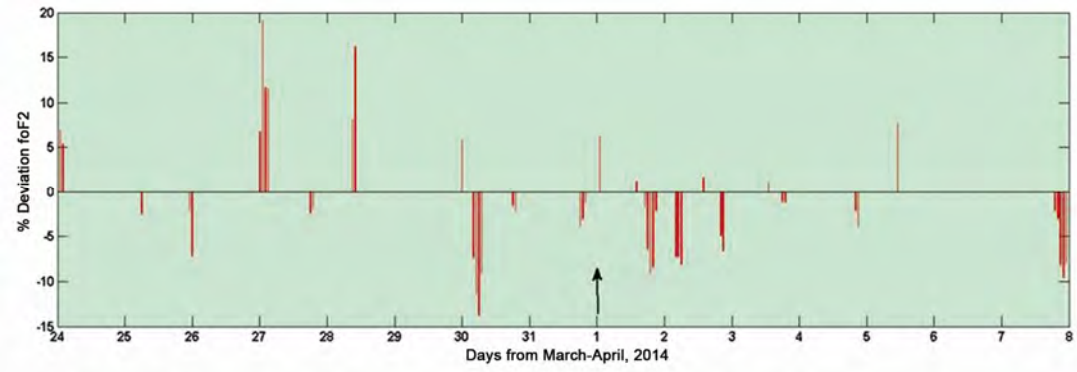

Fig. 6 – The percentage of foF2 deviation for the equivalent observation period presented in Fig. 5. The positive and negative values of the filtered foF2% presents the variation with respect to the UB and LB, respectively

21LT to 24LT (LT=UT-3hr) which may be the source of the extreme positive enhancement (16%).

3.3 Investigation of the ionospheric disparities of 24 June, 2011 Fox island earthquake

June 24, 2011 Fox island (52.00°N, 171.85°W) at Alaska tremor, of magnitude 7.2 in Richter scale at 03:09 UTarose (shown in Table 1) because of tectonic fault within the down-going Pacific slab, as it plunges underneath the North America plate near the Aleutian Trench, in the subduction zone spreading to the southwest from Alaska. Yet, June 24 earthquake is close to the subduction thrust edge in the region, its depth (currently projected as 63 km) and mechanism (either very thin or steep normal faulting) both

recommend that the earthquake occurred within the subducting plate, outside the down-dip edge of the joined zone between North America and the Pacific. At the position of this event, the Pacific plate congregates with North America at a rate of around 71 mm/y in a northwest direction. The data receiver is located at King Salmon (58.4°N,156.4°W), placed at 1207 km from the epicenter lies in Dobrovolsky zone, as visible in Table 1. Figure 8 depicts the geomagnetic indices Dst, AE, Kp, ap, and the foF2

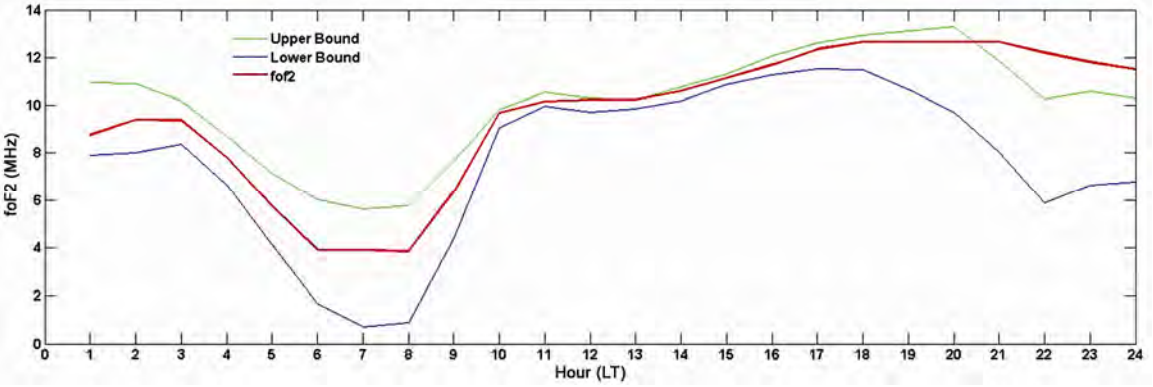

Fig. 7 – LT discrepancies in foF2, UB, LB on 28 March, 2014

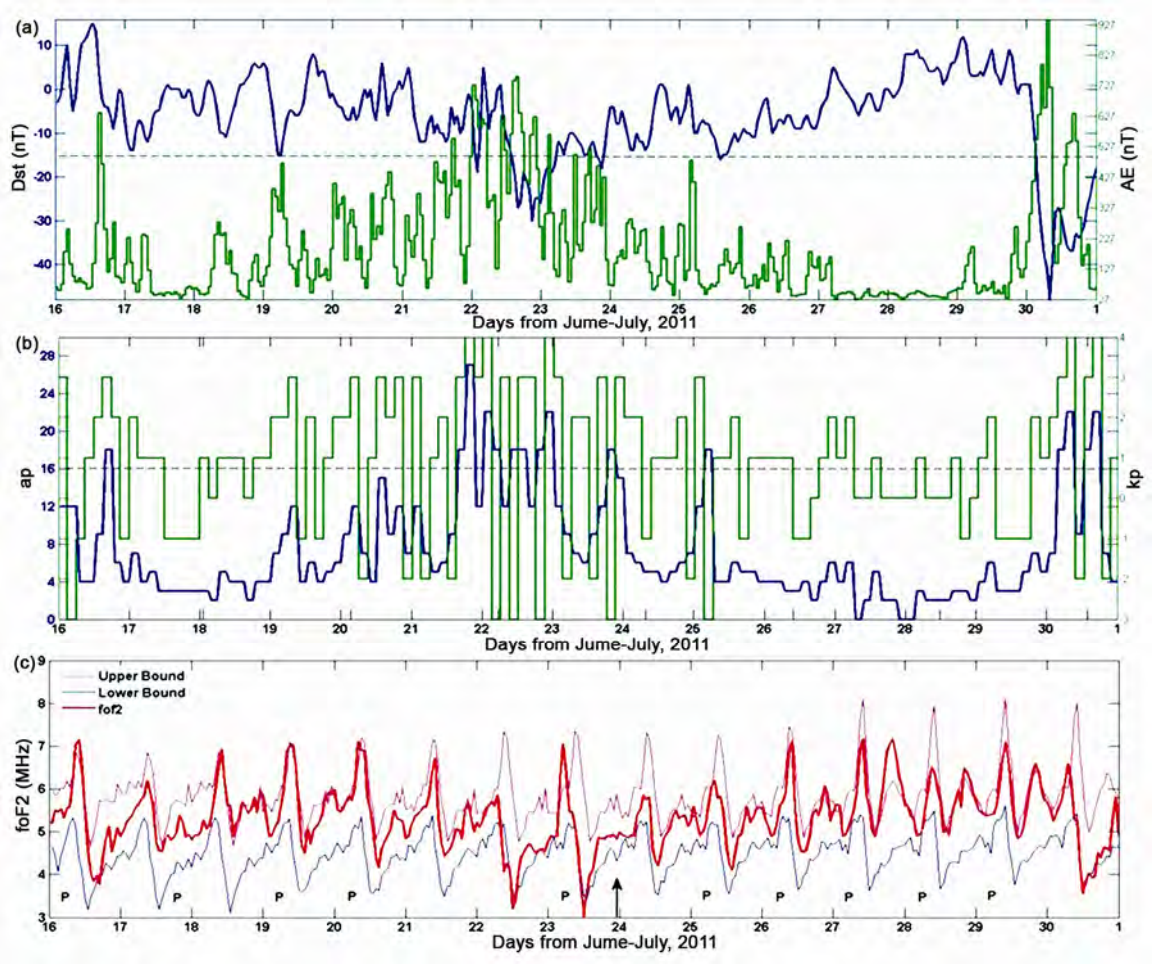

Fig. 8 – The geomagnetic indices (a) Dst and AE, (b) ap and Kp, and (c) foF2 discrepancies and the related UB and LBs between 16 June to 1 July 2011, at the epicenter (52.00°N, 171.85°W), obtained by ionosonde

variants with the associated UB and LBs for our study period between 16 June to 1 July 2011, at data receiver station. The vertical arrow in the figure symbols the time of the earthquake. The horizontal black lines in Fig. 8(a,b) demarcate the threshold values of the Dst and ap indices, which are -15 nT and 16, respectively. In Fig. 8(c), foF2 signal derived from ionosonde with the UB and LBs are plotted using the technique conversed in Section 3. The foF2 signal was not successful to outdo the LB in Fig. 8(c), but it overdoes the UB. The detections were seen between the period of 7 days pre and post tremor activity at the neighborhood of the epicenter. However, as flagged by the Dst, AE, Kp and ap indices in Fig. 8(a,b), the geomagnetic activities during the days of 17, 19, 20, 21, 24 and 26 to 30 June were considered as quiet, therefore, only foF2 variances observed on these days are well-thought-out as possible pre-earthquake ionospheric anomalies, hence they are highlighted by the *P* character and no anomaly is found on disturbed days as delineate in Fig. 8(c). Figure 9 displays the percentage of foF2 deviation for the same observation period presented in Fig.8 In this figure the positive and negative values of the filtered foF2% make out the discrepancy with respect to the UB and LB, respectively. The significant increases in ΔfoF2% in Fig. 9 is about 1–16% were observed on a number of days with respect to Fig. 8(c). Extreme crest intensification (16%) had appeared on 28 June, 2011 after 4th day of the EQ occurrence day. LT disparities in the ionosphere of this earthquake of 28 June is plotted in Fig. 10, which depicts foF2 curve ahead the UB curve from 8LT to 15LT (LT=UT-8hr) which may be the root of extreme amplification on same day in Fig.10.

3.4 Analysis of the ionospheric dissimilarities of the 24May, 2014Greece seismic activity

The Greece quake also known as Aegean sea earthquake located to the south island of Samothraki, Greece (40.28°N, 25.38°E) having depth 6.4 km, occurred at 09:25 UT as the result of strike-slip faulting at shallow depths below the northern Aegean Sea. Primary faulting mechanisms for the event specify slip appeared on a SSE-NNW inclining left-lateral fault, or on a WSW-ENE leaning towards right lateral structure. The position of the tremor and orientation of the WSW-ENE nodal plane are reliable

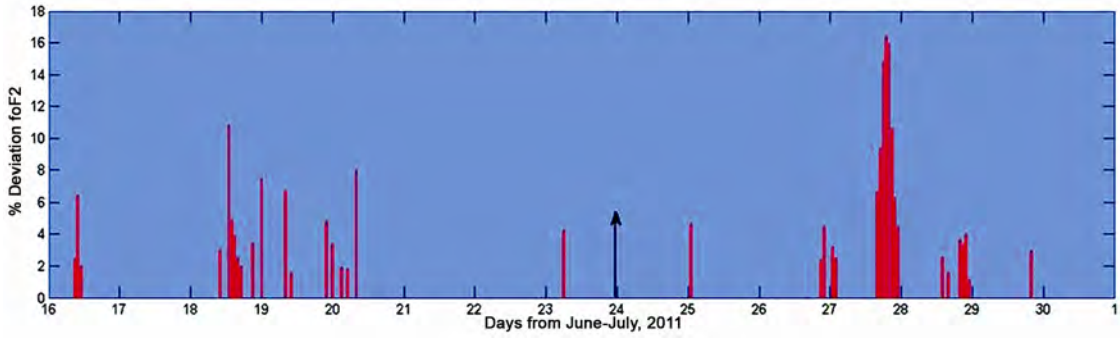

Fig. 9 – At the epicenter (52.00°N, 171.85°W), the percentage of foF2 deviation between 16 June to1 July, 2011. The positive values illustrate the filtered ΔfoF2% variations with respect to the UB derived from ionosonde

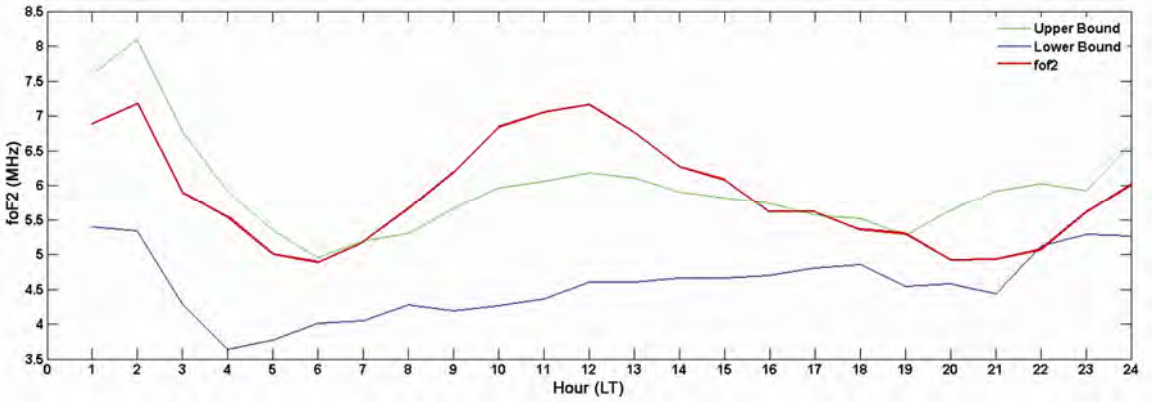

Fig. 10 – LT changes in foF2, UB, LB on 28 June, 2011

with right-lateral faulting within the North Aegean Furrow. Faults within the North Aegean Crib signify the branch of the North Anatolian fault structure, the major transform faulting structure in northern Turkey along with the westward push of the Anatolian microplate with respect to Eurasia, at a rate of around 25 mm/y. The data receiver is located at Athens (38.0°N, 23.5°E) positioned at 301 km from the epicenter lies in Dobrovolsky zone, as illustrated in Table 1. Figure 11 presents the geomagnetic indices Dst, AE, Kp, ap, and the foF2 departure with the associated UB and LB for the observation period between 16-31 May, 2014, at data receiver station. The vertical arrow in the Figure points the time of the earthquake. The horizontal black lines in Fig. 11(a,b) directs the threshold values of the Dst and ap indices, which are -15 nT and 16, respectively. In Fig. 11(c), foF2 signal derived from ionosonde with the UB and LB are plotted using the method conversed in Section 3. The foF2 signal was fruitful to outstrip the UB and LB in Fig. 11(c). The detections were seen between the period of 7 days pre and post tremor activity at the neighborhood of the epicenter. However, as indicated by the Dst, AE, Kp and ap indices in Fig. 11(a–b), the geomagnetic conditions during the 23 May, 2014 was disturbed, while the geomagnetic levels on 17, 18, 19, 21, 24-31 May were characterized as quiet. Therefore, only foF2 anomalies observed on for these days are considered as possible pre-earthquake ionospheric anomalies, hence they are highlighted by the *P* character and the ones seen on disturbed days are highlighted by the *D* character as depicted in Fig. 11(c). Figure 12 displays the percentage of foF2 deviation for the same observation period presented in Fig. 11. In this Figure, the positive and negative value of the filtered foF2% exhibits the discrepancy with respect to the UB and LB, respectively. Referring to the days which manifests developments in Fig. 12, are found the significant increase in ΔfoF2% of about 1–26.6% were observed on 17, 18, 19, 21, 24-31 May

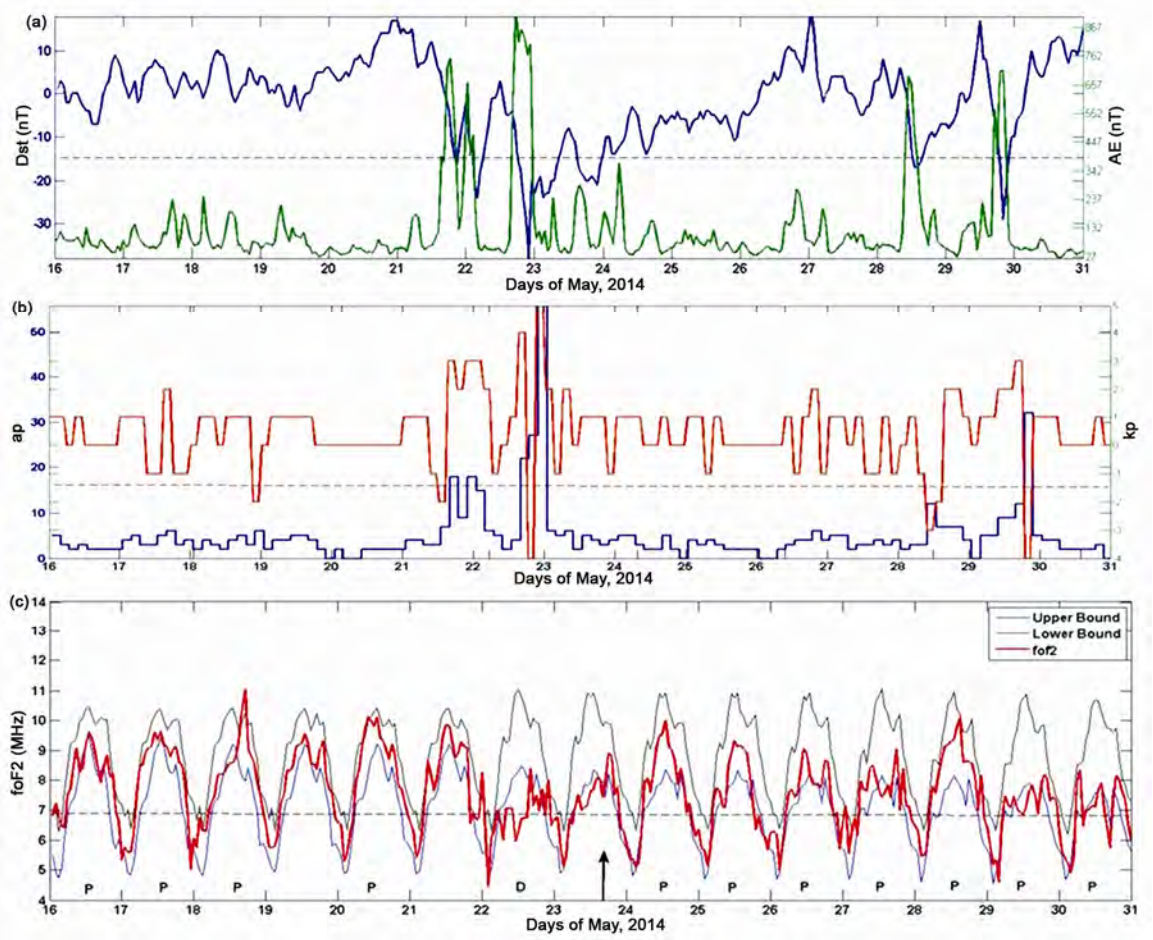

Fig. 11 – The geomagnetic indices (a) Dst and AE, (b) ap and Kp, and the (c) foF2 discrepancies and the related UB and LBs between 16 to 31 May 2014, at the epicenter (40.28°N, 25.38°E), obtained by ionosonde

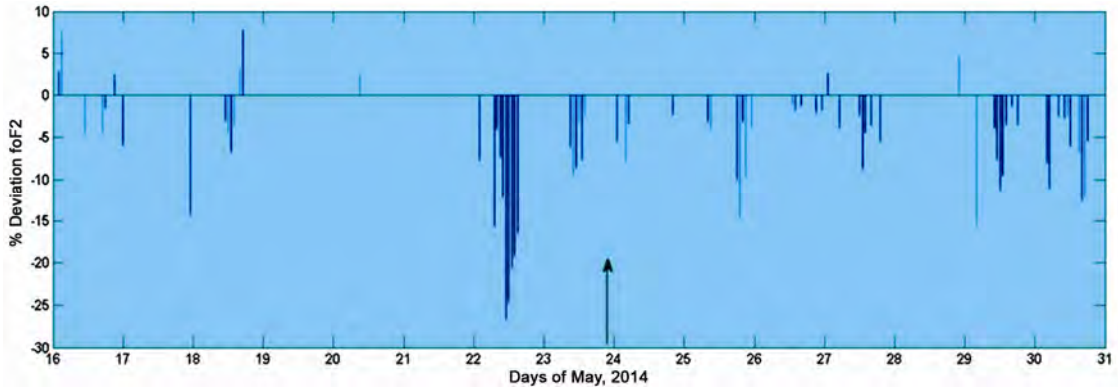

Fig. 12 – At the epicenter (40.28°N, 25.38°E), the percentage of foF2 deviancy between 16 to 31 May, 2014. The positive and negative values present the filtered ΔfoF2% fluctuations with respect to their UB and LB, derived from ionosonde

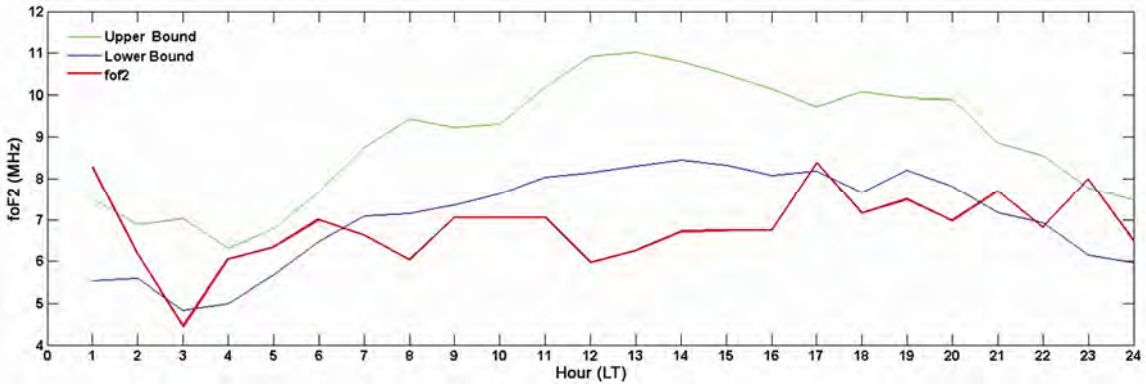

Fig. 13 – LT distinctions in foF2, UB, LB on 23 May, 2014

with respect to Fig. 11(c). Extreme trough intensification (26.6%) had appeared on 23 May, 2014, 1 day before the earthquake manifestation. LT deviation in the ionosphere for this earthquake, on 23 May, 2014 is plotted in Fig. 13, which depicts foF2 plot descend below to the LB in three different time slot for instance at 3LT (LT=UT+2hr) after that from 7LT to 16LT and at last from 18LT to 20LT which covered most part of the day.

4. Discussions

In this paper, we put our efforts to study the main characteristic trait of the seismo-ionospheric distinctions derived from ionosonde data measured at mid and low latitude. Here we are discussing the cause of seismo-ionospheric effect and trying to explain the physics of how the ionosphere starts the sensation of an earthquake. There are numerous Geo-electric fluctuations prevailing due to several geophysical phenomenon's[36] in seismically vigorous areas. It is established that, due to anisotropy of atmospheric conductivity at altitudes more than 60 km, a high intense vertical electric field is created at seismically active zones a few days prior to the earthquakes which can pierce into the ionosphere and generate precise irregularities of electron concentration in this region[37]. This takes place when the size of the range on the ground surface employed by the anomalous field surpasses 200 km in diameter which obey the Dobrovolsky *et al.*[30] formula for earthquake preparatory zone. As all the earthquakes analysed at low and mid latitude are in this zone a high electric field is created which further causes fluctuating electron densities and variations in foF2. So the anomalous quasi-static electric field produced on the ground surface in a seismo-active area is diagnosed through the seismogenic dissimilarities in the near-Earth plasma due to the high conductivity beside the geomagnetic field lines. This is possibly demonstrated in many physical parameters of space plasma measured by onboard satellites/receivers at various stations. In low and mid Latitude, the vertical drift of the F2 region ionospheric plasma under the effect of zonal electric fields produced due to quake activity was proposed by Namgaladze *et al.*[38]. Calculations were carried out using the upper

atmosphere model (UAM), which is a global numerical model of the Earth's upper atmosphere. In this model, the ionospheric response to the accomplishment of zonal electric fields of seismogenic foundations at low latitude was examined by switching on the electric field sources in the UAM electric potential equation. These electric fields in line may disrupt the ionosphere F-2 electron density[39,40]. It was hence unfolded that the action of the near equatorial source expands the equator anomaly in the near-epicentral region of the ionosphere at the magnetic equator and displacing the peaks from the equator to the middle latitudes, further causing anomalies. An electrodynamical model for atmosphere-ionosphere coupling was recommended by Sorokin *et al.*[41] along with Sorokin & Chmyrev[42]. The theoretical model of the conductivity-current spreading in the atmosphere and ionosphere, instigated by external electric current was formulated by Sorokin *et al.*[43]. Conferring to this model the external current initiates due to emanation of charged aerosols transported in the atmosphere by soil gases and the following process of upward transferal, gravitational sedimentation as well as charge relaxation. Further Sorokin *etal.*[44] included the electron-density altitude dispersal in the ionosphere caused by an external current arising in the lower atmosphere in this model. Sorokin & Hayakawa[45] as well as Kuo *et al.*[46] established an enriched coupling model for lithosphere–atmosphere–ionosphere link. There is a propensity of transition from acoustically-driven processes to electric-field coupling[47]. Within the area of the earthquake preparation zone, the seismogenic electric field is formed due to the emission of radioactive particles (radon) into the atmosphere. The anomalous electric field then pierces into the lower ionosphere and thus disrupts the ionosphere. Kim *et al.*[48] first predicted the electric field in the ionosphere which is nearly 1mV/m in a columnar coordinate, for a specified external vertical electric field of 1000 V/m. Nevertheless, the electric field might be overestimated. In the manifestation of a normal vertical electric field of about 100 V/m, Ampferer *et al.*[49] & Xu *et al.*[50] found a rather weak electric field of micro V/m in the ionosphere, due to the low conductivity of the atmospheric layer. The ground vertical electric field should be of 10^5 mV/m, to produce an electric field of mV/m in the ionosphere, which is still not seen. A distinctive ionospheric contextual electric field of 1mV/m is dominantly induced by neutral air wind, i.e., $E = V \times B$, will produce a plasma drift velocity of about 40m/s in the equatorial ionosphere through the effect of $E = V \times B$. Hence, the micro V/m electric field only leads to 0.04m/s drift velocity, which need not be careful in investigating ionospheric distinction[50]. Sorokin & Hayakawa[45] attained some mV/m electric field in the ionosphere by familiarizing an external current, *Je*, produced by charged aerosols inserted into the atmosphere and keeping the aggregate current divergence-free; $J + Je = 0$. Recently, Pulinetsn & Davidenko[47] disbelief the existence of charged aerosols. They anticipated the concept of the Global Electric Circuit (GEC) by providing a reasonable elucidation of the anomalous electric field in the ionosphere, due to the declining atmospheric conductivity and the growing ionospheric potential. But, Omori *et al.*[51] claimed that the radon release amplified the number density of insignificant ions and the atmospheric conductivity, subsequently diminishing the atmospheric electric field, an opinion also pooled by Harrison *et al.*[52]. As centered on the electro dynamic model and discussions, we can conclude that the inoculation of vigorous substances for instance radon gas and products of its decay over the tremor preparation zone varies the altitude sketch of the electrical conductivity of the atmosphere. Too convective transport of charged aerosols in the lower atmosphere at altered platforms of earthquake progress leads to the formation of an external electric current. Its penetration in the atmosphere-ionosphere electric circuit is due to the strengthening of the conductivity current those energies into the ionosphere to distress it during the quake preparation. Actually the processes begin from tectonic plates and the stress of these tectonic plates are the roots of discharge of energy, which is the primary stage for the earthquake preparation and describes the discharge of radon and other gases causes the origination of the acoustic gravity waves[3]. The acoustic gravity waves cause inconsistent electric field generation, further modifying the electron density which is a possible source of causing variations in foF2. The origination of acoustic gravity generation can be clarified by Irwin & Barnes[53]. They claimed the carbon dioxide releases takes place with the seismic activity may specify the high pore pressure in the crust as well as potential seismic areas. The CO_2 discharges have regular character at tectonic faults because ofthermal crustal irregularities but at

times they are not witnessed. In such condition, helium-enriched nitrogen is identified in seismic prone areas[54]. The enormous flows of gas can transport with them supplementary substances that are shaped duringthe morphology transformation course before the occurrence of earthquake taking the form of aerosols. If the volume of these arising gases from tectonic crack is quiet large, they directly cause the origination of an anomalous electric field. In this way, this anomalous electric field interacts with the ionosphere further causing large scale change (together enhancement and depletion) in the electron density. Maximum positive enhancement of 34% and 19% is detected in Sumatra and Chile region tremors, respectively, which are in low latitude. In the mid latitude earthquakes extreme negative enhancement is witnessed at Greece (26%) whereas extreme positive peak for Fox Island (16%) is seen. In these four cases extreme heighteningof anomalies for low latitude earthquakes as compared to mid latitude tremors isidentified. The foF2 variations are extreme in Sumatra as compared to the variations of Greece, Fox Island and Chile. As the magnitude of Sumatra is maximum, there is a possibility of increased preearthquake ionospheric anomalies. This result is in line with the work of Liu *et al.*[55] who statistically probed the association between foF2 variations in Taiwan region for 184 earthquakes with magnitude $M \geq 5.0$ and established that the numbers of earthquakes with pre earthquake ionospheric anomaliesenhances with the earthquake magnitude. The maximum anomaly obtained at Sumatra can be interpreted as it lies near to the equator, the equatorial anomaly (EA) is seen which is a consistent phenomenon of the ionosphere. EA expresses itself as an extreme electron concentration through the geomagnetic equator with two peaks (15–20˚) north and south of it. During quiet conditions, the EA structure starts in the mid-morning hours, reaches its maximum enlargement in the noon and then slowly vanishes in the evening and night. At night, the EA crests shift towards equator and thus the maximum electron density at the geomagnetic equator is restored. EA is very sensitive to any changes in electric fields. Reports regarding the EA modification structure prior to low-latitude and equatorial earthquakes was given by Liu *et al.*[56], Pulinets & Lagen'ka[57], Zakharenkova *et al.*[58]. The chief features of the modification are manifested in the daytime EA amplification near the epicenter. To verify that these anomalies in four earthquakes arise due to seismic activity, we have chosen onecase which is Sumatra earthquake for our analysis. Estimations were done in the same span of observations during pre and post shock happening years which are non-seismic periods. Comparison results of the obtained anomalies with respect to the percentage deviation of foF2 in 2011, 2012 and 2013 confirms that anomalies prevail in the ionosphere for few days due to the happening of earthquake which are pre and post shock days. The extreme anomaly seen in 2013 may be due to travelling ionospheric disturbances (TIDs) or some other prevailing factors in the ionosphere as the solar cycle was minimum. The other anomalies identified during quiet period in 2011 and 2013 may be due to other geophysical factors. By similar analogy, calculations infer that the anomalies seen in the ionosphere for other three events are due to earthquake occurrence.

5 Conclusions

Based on the present examinations, the main features of this study are listed below:

(i) By diagnosing the data of four earthquakes, two from mid latitude and two from low latitude during 2011-2014, in the light of magnetic storms and earthquakes, we saw that the anomalous discrepancies in foF2 are soundly correlated with the existences of high magnitude earthquakes that arose within Dobrovolsky range from there, respective epicenters.

(ii) We perceive that out of all four cases comprising of mid and low latitude earthquakes, mutually exhaustions and heightening pop up in three tremors except in one case which is Fox Island earthquake where the enhancements only befallen.

(iii) In all of these four cases the unit of the Dst index was more than -15nT, the kp index less than 3 and the ap index is less than 16, which clearly indicates that there was no geomagnetic storm 7 days pre and post the chief shock of the temblor(i.e. geophysical quiet days). Consequently, we can clinch that all these ionospheric anomalies were the signatures of the earthquakes.

(iv) Extreme positive enhancement is witnessed for both the low latitude and one mid latitude tremor, except Greece earthquake which revealed extreme trough amplification. As we move from

equator towards poles the foF2 variations start declining, irrespective of hemispheres.

(v) In the two cases namely Sumatra Island and Fox Island extreme perturbations are witnessed post the earthquake and in other two places, Greece and Chile anomalies appeared prior the occurrence of events.

(vi) For peak days prolonged LT variants are seen for nine hours in Greece zone, while in other three regions LT disparities exist for three to four hours.

(vii) Night time extreme anomaly was seen only in Chile earthquake, which is in accordance to the report of ionospheric anomalies existing at nighttime[59]. This feature of LT variation in foF2 triggered by earthquakes is in line with the inferences specified by Liu *et al.*[21]. Arithmetical analysis has proved that the earthquake-induced ionospheric incongruities versus LT are utmost repeated in the noon LT zone[21,60] which agrees with the Greece, Fox Island, Sumatra earthquake induced extreme anomalies.

(viii) A possible mechanism based on the seismogenic electric field in the foundation zone of the earthquake has been discussed. To study the mechanism of lithosphere-ionosphere pairing, multi-station measurement, using different instruments at different height levels of the atmosphere is must.

Acknowledgement

We wish to thank World Data Centre Kyoto Japan for providing geomagnetic indices. Authors are very grateful to the site http://www.spidr.ngdc.noaa.gov/ for providing foF2 values. The authors are also thankful to United States Geological Survey (USGS) for accessing earthquake information and MATHSWORK private limited.

References

1 Ezquer R G, López J L, Scidá L A, Cabrera M A, Zolesi B, Bianchi C, Pezzopane M, Zuccheretti E & MosertM, *J Atmos Solar Terr Phys*, 107 (2014) 89.

2 Zhao X, Ning B, Liu L & Song G, *Adv Space Res*, 53 (3) (2014) 387.

3 Pulinets S A & Boyarchuk K A, *Ionospheric precursors of earthquake* (Springer, Berlin Germany), 2004.

4 Molchanov O A & Hayakawa M, *Seismo electromagnetics and related phenomena: History and latest results*, (TerraPub,Tokyo), 2008.

5 Watthanasangmechai K, Supnithi P, Lerkvaranyu S, Tsugawa T, Nagatsuma T & Maruyama T, *Earth Planets Space*, 64 (2012) 473.

6 Klimenko M V, Klimenko V V, Zakharenkova I E & Karpov I V, *Earth Planets Space*, 64 (2012) 441.

7 Tronin A A, Hayakawa M & Molchanov O A, *J Geodyn*, 33 (2002) 519.

8 Liu J Y, Chuo Y J, Shan S J, Tsai Y B, Chen Y I, Pulinets S A & Yu S B, *Ann Geophys*, 22 (2004) 1585.

9 Tramutoli V, Cuomo V, Filizzola C, Pergola N & Pietrapertosa C, *Remote Sens Environ*, 96 (2005) 409.

10 Parrot M, *Transworld Research Network*, (2009) 205.

11 Oyama K I, Kakinami Y, Liu J Y, Abdu M A & Cheng C Z, *J Geophys Res*, 116 (2011).

12 Gokhberg M B, Pilipenko V A & Pokhotelov O A, *Izvestiya Earth Physics*, 19 (1983b) 762.

13 Gokhberg, M B, Gufel'd I L, Marenko V F, Ponomarev E A, Rozhnoy A A & Yampolsky V S, *Izv Phys Solid Earth*, 23 (1987) 102.

14 Gokhberg M B, Morgunov V A & Pokhotelov O A, *Seismo-electromagnetic phenomenana*, (Moscow), 1988.

15 Liperovsky V A , Asimov O A, Shalimov S A, Gokhberg M B, Liperovskaya R H & Saidshoev A, *Physics Solid Earth*, 12 (1990) 77.

16 Pulinets S A, Legen'ka A D, Gaivoronskaya T V & Depuev V K, *J Atmos Sol Terr Phy*, 65 (2003) 337.

17 Ondoh, *Adv Space Res*, 26 (2000) 1267.

18 Rios V H, Kim V P & Hegai V V, *Adv Space Res* 33 (2004) 323.

19 Singh B, Kushwah V, Singh O P , Lakshmi D R & Reddy B M , *J Phys Chem Earth*, 29 (2004) 537.

20 HobaraY& Parrot M, *J Atmos Sol Terr Phy*, 67 (2005) 677.

21 Liu J Y, Chen Y I, Chuo Y J & Chen C S, *J Geophys Res*, 115 (2006) A09312.

22 Liu J Y, Chen Y I, Pulinets S A, Tsai Y B & Chuo Y, *J Geophys Res Lett*, 27 (2000) 3113.

23 Le H, Liu J Y & Liu L, *J Geophys Res*, 116 (2011) A09307.

24 Zelenova T I & Legen'ka A I, *Earth Physics*, 25 (1989) 848.

25 Forbes J M, Palo S E & Zhang X, *J Atmos Sol Terr Phy*, 62 (2000) 685.

26 Rishbeth H & Mendillo M, *J Atmos Sol Terr Phy*, 63 (2001) 1661.

27 Mendillo M, Rishbeth H, Roble R G & Wroten J, *J Atm Sol Terr Phys*, 64 (2002) 1911.

28 Sojka J, David M, Schunk R W & Heelis R A, *J Geophys* Res, 117 (2012) A02315.

29 Kumar S, Priyadarshi S, Seemala G K & Singh A K, *Astrophys Space Sci*, 339 (2012) 165.

30 Dobrovolsky I R, S I Zubkov & Myachkin V I, *Pure Appl Geophys*,11 (1979) 1025.

31 Xu T, Hu Y L, Wang F F, Chen Z & Wu J, *Ann Geophys*, 33 (2015) 687.

32 Dabas R S, Das R M, Sharma K & Pilai K G M, *J Atmos Sol Terr Phy*, 69 (2007) 1813.

33 Zakharenkova I E, Shagimuratov I I, Krankowski A & Lagovsky A F, *Stud Geophy Geod*, 51 (2007) 267.

34 Gonzalez W D, Joselyn J A, Kamide Y, Kroehl H W, Rostoker G, Tsurutani B T & Vasyliunas V M, *J Geophys Res*, 99 (1994) 5771.

35 Osella A, Favetto A & Silbergleit V, *J Atmos Terr Phys*, 59 (1997) 445.

36 Telesca L, Colangelo G, Hattori K & Lapenna V, *Nat Hazards Earth System Sci*, 4 (2004) 663.

37 Pulinets S A, Legen'ka A D & Zelenova T I, *Geomagn Aeronomy*, 38 (1998) 400.

38 Namgaladze A A, Shagimuratov I I, Zakharenkova I E, Zolotov O V & Martynenko O V, *XXIV IUGG General Assembly* (Perugia, Italy),02–13 July 2007.

39 Namgaladze A A, Klimenko M V, Klimenko V V & Zakharenkova I E, *Geomagn Aeronomy*, 49 (2009) 252.

40 Namgaladze A A, Zolotov O V, Zakharenkova I E, Shagimuratov I I & Martynenko O V, *Proceeding of the MSTU*, (2009) 308.

41 Sorokin V M, Chmyrev V M &Yaschenko A K, *J Atm Sol Ter Phys*, 63 (2001) 1681.

42 Sorokin V M & Chmyrev V M, *Geomagn Aeronomy*, 42 (2002) 784.

43 Sorokin V M, Chmyrev V M &Yaschenko A K, *J Atm Sol Ter Phys*, 67 (2005) 1259.

44 Sorokin V M, Yaschenko A K & Hayakawa M, *J Atmos Sol Terr Phy*, 68 (2006) 1260.

45 Sorokin V & Hayakawa M, *Appl Sci*, 7 (2013) 1.

46 Kuo C L, Lee L C & Huba J D, *J Geo phys Res*, 119 (2014) 3189.

47 Pulients S A & Davidenko D, *Adv Space Res*, 53 (2014) 709.

48 Kim V P, Khegai V V & Illich-Svitych P V, *Phys Solid Earth*, 30 (1994) 223.

49 Ampferer M, Denisenko V V, Hausleitner W, Krauss S, Stangl G, Boudjada M Y & Biernat H K, *Ann Geophys*, 28 (2010) 779.

50 Xu T, Zhang, H, Hu Y L & Wu J, *Adv Space Res*, 55(2015) 2883.

51 Omori Y, Yasuoka Y, Nagahama H, Kawada Y, Ishikawa T, Tokonami S & Shinogi M, *Nat Hazards Earth System Sci*, (2007) 629.

52 Harrison R G, Aplin K L & Rycroft M J, *J Atmos Solar Terr Phys*, 72 (2010) 376.

53 Irwin W P & Barne I, *J Geophy Res*, 85 (1980) 3115.

54 Toutain J P & Baubron J C, *Tectonophysics*, 304 (1998) 1.

55 Liu J, Tsai Y, Ma K, Chen Y, Tsai H, Lin C, Kamogawa M & Lee C, *J Geophys Res*, 111 (2006) A05303.

56 Liu J Y, Chuo Y J, Pulinets S A, Tsai H F & Zeng X P, *Terrapub*), (2002) 297.

57 Pulinets S A & Legen'ka A D, *Geomagn. Aeronomy*, (2002) 227.

58 Zakharenkova I E, Shagimuratov I I, Tepenitzina, Yu N & Krankowski A, *J Atmos Sol Terr Phy*, 70 (2008) 1919.

59 Zakharenkova I E, Krankowski A & Shagimuratov I I, *Nat Hazards Earth System Sci*, 6 (2006) 817.

60 Sharma K, Dabas R S, Sarkar S, Das R M, Ravindran S & Gwal A K, *J Geophys Res*, 115 (2010).